Scientific paper

Insights into Antiradical Behavior: Crystal Structures and DFT Analysis of 2-Formylpyridine N^4 -Allylthiosemicarbazone Salts

Yurii Chumakov¹ , Vasilii Graur^{2,*} , Ianina Graur² , Victor Tsapkov² , Olga Garbuz^{2,3} and Aurelian Gulea²

¹ Institute of Applied Physics, Moldova State University, Academiei 5, MD2028 Chisinau, R. Moldova

² Laboratory of Advanced Materials in Biopharmaceutics and Technics, Moldova State University, Mateevici 60, MD2028 Chisinau, R. Moldova

³ Laboratory of Systematics and Molecular Phylogenetics, Institute of Zoology, Moldova State University, Academiei 1, MD2028 Chisinau, R. Moldova

* Corresponding author: E-mail: vgraur@gmail.com

Received: 03-03-2024

Abstract

In this paper, six new salts of 2-formylpyridine N^4 -allylthiosemicarbazone ([H₂L]X·nH₂O, where X is NO₃⁻(1), NH₂SO₃⁻(2), Cl⁻(3), Cl₃CCOO⁻(4), Cl₂CHCOO⁻(5), ClCH₂COO⁻(6); n = 0 (1, 3, 5, 6), 1 (2, 4)) were synthesized and physico-chemically characterized by elemental analysis, molar conductivity measurements, FT-IR studies, ¹H and ¹³C NMR. The crystal structures of compounds 1–5 were determined by single-crystal X-ray diffraction. Crystal data analysis shows that the structures of these compounds consist of protonated thiosemicarbazone $\mathbf{H}_2\mathbf{L}^+$, anions of acid residue, and water molecules in 2 and 4. These compounds manifest antiradical activity toward ABTS⁺⁺ cation radicals that exceeds the activity of non-protonated thiosemicarbazone $\mathbf{H}_2\mathbf{L}$ and Trolox used in medical applications. The most active one is compound [H₂L]Cl (3) with an IC₅₀ value of 9.9 µmol/L. Density Functional Theory calculations showed that the electronic structure of cation $\mathbf{H}_2\mathbf{L}^+$ is more favorable for accepting electron if compared with $\mathbf{H}_2\mathbf{L}$.

Keywords: Crystal structure, thiosemicarbazone, theoretical calculation, antiradical activity

1. Introduction

Normal cellular metabolism consistently generates reactive oxygen species. For example, during respiration, our cells convert oxygen to water. Sometimes, a portion of this oxygen escapes the complete transformation resulting in the formation of a highly reactive oxygen species known as the superoxide anion. Additional free radicals, such as hydrogen peroxide (HOO•) and nitric oxide (NO•), arise from diverse chemical reactions within our organism. Enzymatic or biochemical defense mechanisms typically remove these highly reactive molecules. There are also systems for repairing the detrimental effects caused by free radicals. However, when free radicals enter our body under the influence of factors such as smoking, pollution, and stress, the body's system is overloaded. Under such circumstances, the use of external antioxidant supple-

ments may be necessary to reinstate cellular redox homeostasis.⁹

In the design and synthesis of advanced antiradical drugs, thiosemicarbazones constitute a group of compounds with an exceptional pharmacological profile. 10-12 Generally, thiosemicarbazones are produced through the condensation of the respective thiosemicarbazide with aldehydes or ketones. 13 Various derivatives of thiosemicarbazones can be synthesized by incorporating substituents onto the ligand backbone, specifically by introducing substituents on the thioamide and hydrazine nitrogen atoms. Certain structural characteristics crucial for the biological functionality of thiosemicarbazones have been recognized. 14 These include the substitution of sulfur in the thiocarbonyl group with selenium or oxygen, alteration of the attachment point of the thiosemicarbazones moiety in the original aldehyde or ketone, and substitution at the termi-

nal N4 position.^{15,16} Additional factors encompass electron density distributions, the characteristics of substituents, the geometry and symmetry of the initial ligand, metal binding capabilities, solubility, and the potential for interaction with the cell membrane.^{17–20}

2-Formylpyridine thiosemicarbazones and their coordination compounds of some 3d metals were studied as a potential antimicrobial, 21-23, antifungal, 24,25 antitumour,²⁶⁻²⁸ and antioxidant²⁹ agents. Moreover, various biological activities, such as antiproliferative, antibacterial, antifungal, and antiradical have been previously studied for 2-formylpyridine N^4 -allylthiosemicarbazone (HL) and its copper, nickel, cobalt, and zinc complexes.³⁰ In the case of antiradical activity, non-coordinated thiosemicarbazone showed higher activity than most of its metal complexes, and also higher than the activity of the Trolox standard. 2-Formylpyridine N^4 -allylthiosemicarbazone can act as a base and thus can form salts with different acids. Such type of salts is not described in the literature and nothing is known about their antiradical activity.

So, based on all of the above, in this study, new 2-formylpyridine N^4 -allylthiosemicarbazone salts were synthesized, characterized by FT-IR, elemental analysis, nuclear magnetic resonance (NMR), X-ray single crystal diffraction, and their antiradical activity was studied. At the same time, the synthesized compounds were also subjected to density functional theory (DFT) calculation.

2. Experimental Section

2. 1. Materials and Measurements

In this work, all chemical reagents were commercial reagents and have not been further purified. 3-Isothiocyanatoprop-1-ene, hydrazine hydrate, 2-formylpyridine, nitric acid, sulfamic acid, hydrochloric acid, trichloroacetic acid, dichloroacetic acid, and chloroacetic acid were obtained from Sigma-Aldrich and were not additionally purified. The ¹H and ¹³C NMR spectra were recorded on a Bruker DRX-400. Chemical shifts are measured in ppm

relative to tetramethylsilane. CDCl₃ and DMSO- d_6 were used as solvents. FTIR spectra were obtained for powders on a Bruker ALPHA FTIR spectrophotometer at room temperature in the range of 4000–400 cm⁻¹. Elemental analysis was performed similar to the literature procedure. The resistance of solutions of the synthesized salts in DMF (20 °C, c 0.001 M) was measured using an R-38 rheochord bridge.

N-(Prop-2-en-1-yl)hydrazinecarbothioamide (N4-allyl-3-thiosemicarbazide) was synthesized by the reaction between 3-isothiocyanatoprop-1-ene (allyl isothiocyanate) and hydrazine hydrate. ³²

2. 2. Synthesis of the Studied Substances

The compounds **1–6** were prepared by two steps as shown in Scheme 1. First, 2-formylpyridine N^4 -allylthiosemicarbazone was obtained by the method described in the literature. N⁴-Allyl-3-thiosemicarbazide (20.0 mmol, 2.62 g) and 2-formylpyridine (20.0 mmol, 2.14 g) were mixed in 50 mL of 96% ethanol and stirred for about 1 h. The obtained pale-yellow precipitate was filtered, washed with a small amount of ethanol, and dried in air.

Second, the corresponding salts of 2-formylpyridine N^4 -allylthiosemicarbazone were obtained. 2-Formylpyridine N^4 -allylthiosemicarbazone (1.0 mmol, 0.22 g) and an equimolar amount of corresponding acid (1.0 M solution of HNO₃, NH₂SO₃H in water, 1.0 M solution of HCl, Cl₃CCOOH, Cl₂CHCOOH, ClCH₂COOH in water) were mixed in 25 mL of 96% ethanol and stirred for about 40 min on heating. Then, after cooling the corresponding salts of various shades of yellow crystallized from the solutions, were isolated by filtration, washed with ethanol and dried in air.

2-({2-[(Prop-2-en-1-yl)carbamothioyl] hydrazinylidene}methyl)pyridin-1-ium Nitrate [H₂L]NO₃ (1)

Yield: 0.20 g (71%). M. p. 159–160 °C. Anal. Calcd. for $C_{10}H_{13}N_5O_3S$: C, 42.39; H, 4.63; N, 24.72; S,

Scheme 1. Synthesis of the compounds 1-6.

11.32. Found: C, 42.26; H, 4.57; N, 24.68; S, 11.27. FT-IR (KBr, cm⁻¹) v 3240, 3131, 3091 (N-H), 1641 (C=C)_{allyl}, 1619, 1578 (C=N), 1318 (C=S). ¹H NMR (Figure S1) (CDCl₃, 400 MHz) δ 12.30 (br, 1H, NH), 9.17 (br, 1H, NH), 8.83 (d, 1H, CH arom.), 8.46 (m, 2H, CH arom.), 8.16 (s, 1H, CH=N), 7.86 (d, 1H, CH arom.), 5.93 (m, 1H, CH allyl), 5.17 (dd, 2H, CH₂=C), 4.28 (m, 2H, CH₂-N). ¹³C NMR (Figure S2) (CDCl₃, 100 MHz) δ 178.28 (C=S), 148.53, 134.54, 126.27, 124.90, 124.84 (C arom), 144.44 (C=N azometh.), 134.82 (CH allyl), 116.50 (CH₂=), 46.42 (CH₂-N). λ (DMF, Ω^{-1} ·cm²·mol⁻¹) 83.

2-($\{2-[(Prop-2-en-1-yl)carbamothioyl]$ hydrazinylidene $\}$ methyl)pyridin-1-ium Sulfamate Hydrate $[H_2L]SO_3NH_2\cdot H_2O$ (2)

Yield: 0.25 g (75%). M. p. 173–174 °C. Anal. Calcd. for $C_{10}H_{17}N_5O_4S_2$: C, 35.81; H, 5.11; N, 20.88; S, 19.12. Found: C, 35.76; H, 5.06; N, 20.79; S, 19.05. FT-IR (KBr, cm⁻¹) ν 3428, 3365, 3285, 3188, 3085 (N–H), 1643 (C=C) $_{allyl}$, 1617, 1582 (C=N), 1320 (C=S). λ (DMF, Ω^{-1} · cm²·mol⁻¹) 88.

2-({2-[(Prop-2-en-1-yl)carbamothioyl] hydrazinylidene}methyl)pyridin-1-ium Chloride [H₂L]Cl (3)

Yield: 0.19 g (73%). M. p. 159–160 °C. Anal. Calcd. for $C_{10}H_{13}ClN_4S$: C, 46.78; H, 5.10; Cl, 13.81; N, 21.82; S, 12.49. Found: C, 46.68; H, 5.05; Cl, 13.75; N, 21.77; S, 12.40. FT-IR (KBr, cm⁻¹) ν 3190, 3116, 3098 (N–H), 1646 (C=C)_{allyl}, 1615, 1574 (C=N), 1312 (C=S). λ (DMF, Ω^{-1} · cm²·mol⁻¹) 66.

2-({2-[(Prop-2-en-1-yl)carbamothioyl] hydrazinylidene}methyl)pyridin-1-ium Trichloroacetate Hydrate [H₂L]Cl₃CCOO·H₂O (4)

Yield: 0.3 g (74%). M. p. 138–139 °C. Anal. Calcd. for $C_{12}H_{15}Cl_3N_4O_3S$: C, 35.88; H, 3.76; Cl, 26.48; N, 13.95; S, 7.98. Found: C, 35.78; H, 3.68; Cl, 26.40; N, 13.85; S, 7.89. FT-IR (KBr, cm $^{-1}$) v 3336, 3146, 3084 (N–H), 1643 (C=C) $_{allyl}$, 1614, 1582 (C=N), 1314 (C=S). λ (DMF, Ω^{-1} cm 2 ·mol $^{-1}$) 72.

2-({2-[(Prop-2-en-1-yl)carbamothioyl] hydrazinylidene}methyl)pyridin-1-ium Dichloroacetate [H₂L]Cl₂CHCOO (5)

Yield: 0.26 g (76%). M. p. 126–127 °C. Anal. Calcd. for $C_{12}H_{14}Cl_2N_4O_2S$: C, 41.27; H, 4.04; Cl, 20.30; N, 16.04; S, 9.18. Found: C, 41.20; H, 3.94; Cl, 20.24; N, 15.96; S, 9.10. FT-IR (KBr, cm⁻¹) v 3234, 3121, 3079 (N–H), 1645 (C=C)_{allyl}, 1602, 1572 (C=N), 1315 (C=S). λ (DMF, Ω^{-1} · cm²·mol⁻¹) 63.

2-({2-[(Prop-2-en-1-yl)carbamothioyl] hydrazinylidene}methyl)pyridin-1-ium Chloroacetate [H₂L]ClCH₂COO (6)

Yield: 0.23 g (73%). M. p. 128–129 °C. Anal. Calcd. for $C_{12}H_{15}ClN_4O_2S$: C, 45.79; H, 4.80; Cl, 11.26; N, 17.80; S, 10.19. Found: C, 45.58; H, 4.86; Cl, 11.17; N, 17.67; S, 10.10. FT-IR (KBr, cm⁻¹) ν 3252, 3133, 3084 (N–H), 1644 (C=C)_{allyl}, 1612, 1581 (C=N), 1317 (C=S). λ (DMF, Ω^{-1} · cm²·mol⁻¹) 61.

2. 3. X-Ray Crystallography

Single-crystal X-ray diffraction measurements of compounds 1-5 have been carried out on an Xcalibur E charge-coupled device (CCD) diffractometer equipped with a CCD area detector and a graphite monochromator utilizing MoKa radiation at room temperature. Final unit cell dimensions were obtained and refined on an entire data set. All calculations necessary to solve the structures and to refine the proposed model were carried out with the SHELXS97 and SHELXL2015 program packages.^{34–36} The nonhydrogen atoms were treated anisotropically (full-matrix least-squares method on F^2). The H atoms were placed in calculated positions and were treated using riding model approximations with $U_{iso}(H) = 1.2U_{eq}(C)$ and $U_{iso}(H) = 1.5 U_{eq}(O)$. The disordered allyl groups, solvent molecules, and Cl₃CCOO⁻ anion were found in compound 4. The X-ray data and the details of the refinement of studied compounds are summarized in Table 1, and the selected bond lengths, angles as well as hydrogen bond parameters are given in Tables S1, 2. The geometric parameters were calculated by PLATON program³⁷ and Mercury software³⁸ was used for visualization of structures. The hydrogen atoms that were not involved in the hydrogen bonding were omitted from the generation of the packing diagrams.

2. 4. Antiradical Evaluation

The ABTS*+ method³⁹ was utilized to assess the antiradical activity of the substances **1–6**. Procedures for preparing standard solutions of ABTS*+ radical cation, as well as the studied substances, along with the spectrophotometric measurement conditions and inhibition calculations, were made as described.⁴⁰ To create 10 mM stock solutions of the compounds **1–6** and the reference compound (Trolox), 10μ mol of each compound were dissolved in 1 mL of DMSO. Subsequent solutions of 1, 10, 100, and 1000μ M concentrations were prepared by the dilution of stock solutions with DMSO. Following this, 20μ L of each solution of the tested compounds was transferred to a 96-well microtiter plate, and 180μ L of ABTS*+ working solution was added, resulting in final concentrations of tested compounds 0.1, 1, 10, and 100μ M, respectively.

2. 5. Computational Details

The electronic structure of $\mathbf{H_2L^+}$ has been calculated by Density Functional Theory (DFT) of Gaussian16 suite

Table 1. Crystal data and structure refinement for 1-5.

Identification code	1	2	3
CCDC	2270396	2270395	2270397
Empirical formula	$C_{10}H_{13}N_5O_3S$	$C_{10}H_{15}N_5O_4S_2$	$C_{10}H_{13}ClN_4S$
Formula weight	283.31	333.39	256.75
Temperature/K	293(2)	293(2)	293(2)
Crystal system	monoclinic	orthorhombic	orthorhombic
Space group	$P2_1/c$	$P2_12_12_1$	Pbca
a/Å	5.1190(5)	5.1609(6)	14.4136(13)
b/Å	16.353(2)	16.9338(17)	9.9597(14)
c/Å	15.968(2)	17.463(2)	17.3614(19)
α/°	90	90	90
β/°	90.081(9)	90	90
γ/°	90	90	90
Volume/ų	1336.7(3)	1526.1(3)	2492.3(5)
Z	4	4	8
$\rho_{calc}/g \text{ cm}^{-3}$	1.408	1.451	1.369
μ/mm ⁻¹	0.255	0.371	0.453
F(000)	592.0	696.0	1072.0
Reflections collected	2965	3677	5649
Independent reflections (R_{int})	2054 (0.0359)	2579 (0.0343)	2240 (0.0585)
Data/restraints/parameters	2054/6/172	2579/0/193	2240/0/153
Goodness-of-fit on F^2	1.045	0.961	0.910
R_1 , $wR_2[I \ge 2\sigma(I)]$	0.0948, 0.1933	0.0596, 0.1083	0.0529, 0.0780
R_1 , wR_2 [all data]	0.1670, 0.2270	0.1025, 0.1260	0.1209, 0.0967
$\Delta \rho_{\text{max}} / \Delta \rho_{\text{min}} / e \text{ Å}^{-3}$	0.26/-0.22	0.35/-0.28	0.22/-0.24
Identification code	4	5	
CCDC	2270394	2270398	
Empirical formula	$C_{12}H_{12}Cl_3N_4O_3S$	$C_{12}H_{14}Cl_2$	N ₄ O ₂ S
Formula weight	398.67	349.23	1 2
Temperature/K	293(2)	293(2)	
1			
	monoclinic	triclinic	
Crystal system	monoclinic P2 ₁ /c	triclinic <i>P</i> -1	
Crystal system Space group	$P2_1/c$	P-1	
Crystal system Space group a/Å	<i>P</i> 2 ₁ / <i>c</i> 15.7525(6)	<i>P</i> -1 8.1644(6)	
Crystal system Space group a/Å b/Å	P2 ₁ /c 15.7525(6) 6.8339(2)	P-1 8.1644(6) 8.6556(6)	
Crystal system Space group a/Å b/Å c/Å	P2 ₁ / <i>c</i> 15.7525(6) 6.8339(2) 33.2529(10)	P-1 8.1644(6) 8.6556(6) 11.0961(9)	
Crystal system Space group a/Å b/Å c/Å α/°	P2 ₁ /c 15.7525(6) 6.8339(2) 33.2529(10) 90	P-1 8.1644(6) 8.6556(6) 11.0961(9) 91.468(6)	
Crystal system Space group a/Å b/Å c/Å α/° β/°	P2 ₁ /c 15.7525(6) 6.8339(2) 33.2529(10) 90 95.272(3)	P-1 8.1644(6) 8.6556(6) 11.0961(9) 91.468(6) 93.665(7)	
Crystal system Space group a/Å b/Å c/Å α/° β/° γ/°	P2 ₁ /c 15.7525(6) 6.8339(2) 33.2529(10) 90 95.272(3) 90	P-1 8.1644(6) 8.6556(6) 11.0961(9) 91.468(6) 93.665(7) 100.901(6)	
Crystal system Space group $a/Å$ $b/Å$ $c/Å$ $\alpha/^{\circ}$ $\beta/^{\circ}$ $\gamma/^{\circ}$ Volume/Å 3	P2 ₁ /c 15.7525(6) 6.8339(2) 33.2529(10) 90 95.272(3) 90 3564.6(2)	P-1 8.1644(6) 8.6556(6) 11.0961(9) 91.468(6) 93.665(7) 100.901(6) 767.84(10)	
Crystal system Space group $a/Å$ $b/Å$ $c/Å$ $\alpha/^{\circ}$ $\beta/^{\circ}$ Volume/ $Å^3$	P2 ₁ /c 15.7525(6) 6.8339(2) 33.2529(10) 90 95.272(3) 90 3564.6(2) 8	P-1 8.1644(6) 8.6556(6) 11.0961(9) 91.468(6) 93.665(7) 100.901(6) 767.84(10)	
Crystal system Space group $a/Å$ $b/Å$ $c/Å$ $\alpha/^{\circ}$ $\beta/^{\circ}$ $\gamma/^{\circ}$ Volume/ $Å^3$ Z $\rho_{calc}/g cm^{-3}$	P2 ₁ /c 15.7525(6) 6.8339(2) 33.2529(10) 90 95.272(3) 90 3564.6(2) 8 1.4857	P-1 8.1644(6) 8.6556(6) 11.0961(9) 91.468(6) 93.665(7) 100.901(6) 767.84(10) 2 1.511	
Crystal system Space group $a/Å$ $b/Å$ $c/Å$ $\alpha/^{\circ}$ $\beta/^{\circ}$ Volume/ $Å^3$ Z $\rho_{calc}/g cm^{-3}$ μ/mm^{-1}	P2 ₁ /c 15.7525(6) 6.8339(2) 33.2529(10) 90 95.272(3) 90 3564.6(2) 8 1.4857 0.648	P-1 8.1644(6) 8.6556(6) 11.0961(9) 91.468(6) 93.665(7) 100.901(6) 767.84(10) 2 1.511 0.567	
Crystal system Space group $a/Å$ $b/Å$ $c/Å$ $\alpha/^{\circ}$ $\beta/^{\circ}$ Volume/ $Å^3$ Z $\rho_{calc}/g cm^{-3}$ μ/mm^{-1} $F(000)$	P2 ₁ /c 15.7525(6) 6.8339(2) 33.2529(10) 90 95.272(3) 90 3564.6(2) 8 1.4857 0.648 1629.1	P-1 8.1644(6) 8.6556(6) 11.0961(9) 91.468(6) 93.665(7) 100.901(6) 767.84(10) 2 1.511 0.567 360.0	
Crystal system Space group $a/Å$ $b/Å$ $c/Å$ $\alpha/^{\circ}$ $\beta/^{\circ}$ Volume/ $Å^3$ Z $\rho_{\rm calc}/g~{\rm cm}^{-3}$ $\mu/{\rm mm}^{-1}$ $F(000)$ Reflections collected	P2 ₁ /c 15.7525(6) 6.8339(2) 33.2529(10) 90 95.272(3) 90 3564.6(2) 8 1.4857 0.648 1629.1 13159	P-1 8.1644(6) 8.6556(6) 11.0961(9) 91.468(6) 93.665(7) 100.901(6) 767.84(10) 2 1.511 0.567 360.0 4871	
Crystal system Space group $a/Å$ $b/Å$ $c/Å$ $\alpha/^\circ$ $\beta/^\circ$ $\gamma/^\circ$ Volume/Å 3 Z $\rho_{\rm calc}/g~{\rm cm}^{-3}$ $\mu/{\rm mm}^{-1}$ $F(000)$ Reflections collected Independent reflections ($R_{\rm int}$)	P2 ₁ /c 15.7525(6) 6.8339(2) 33.2529(10) 90 95.272(3) 90 3564.6(2) 8 1.4857 0.648 1629.1 13159 6254 (0.0192)	P-1 8.1644(6) 8.6556(6) 11.0961(9) 91.468(6) 93.665(7) 100.901(6) 767.84(10) 2 1.511 0.567 360.0 4871 2848 (0.01)	38)
Crystal system Space group $a/Å$ $b/Å$ $c/Å$ $\alpha/^\circ$ $\beta/^\circ$ $\gamma/^\circ$ Volume/ $Å^3$ Z $\rho_{\rm calc}/g~{\rm cm}^{-3}$ $\mu/{\rm mm}^{-1}$ $F(000)$ Reflections collected Independent reflections ($R_{\rm int}$) Data/restraints/parameters	P2 ₁ /c 15.7525(6) 6.8339(2) 33.2529(10) 90 95.272(3) 90 3564.6(2) 8 1.4857 0.648 1629.1 13159 6254 (0.0192) 6254/0/4401	P-1 8.1644(6) 8.6556(6) 11.0961(9) 91.468(6) 93.665(7) 100.901(6) 767.84(10) 2 1.511 0.567 360.0 4871 2848 (0.01) 2848/0/199	38)
Crystal system Space group $a/Å$ $b/Å$ $c/Å$ $a/^\circ$ $\beta/^\circ$ $\gamma/^\circ$ Volume/Å 3 Z $\rho_{\rm calc}/$ g cm $^{-3}$ $\mu/{\rm mm}^{-1}$ $F(000)$ Reflections collected Independent reflections ($R_{\rm int}$) Data/restraints/parameters Goodness-of-fit on F^2	P2 ₁ /c 15.7525(6) 6.8339(2) 33.2529(10) 90 95.272(3) 90 3564.6(2) 8 1.4857 0.648 1629.1 13159 6254 (0.0192) 6254/0/4401 1.055	P-1 8.1644(6) 8.6556(6) 11.0961(9) 91.468(6) 93.665(7) 100.901(6) 767.84(10) 2 1.511 0.567 360.0 4871 2848 (0.01) 2848/0/199	38)
Crystal system Space group $a/Å$ $b/Å$ $c/Å$ $a/^\circ$ $\beta/^\circ$ $\gamma/^\circ$ Volume/Å 3 Z $\rho_{\rm calc}/g~{\rm cm}^{-3}$ $\mu/{\rm mm}^{-1}$ $F(000)$ Reflections collected Independent reflections $(R_{\rm int})$ Data/restraints/parameters Goodness-of-fit on F^2 $R_1, wR_2~[I \geq 2\sigma(I)]$	P2 ₁ /c 15.7525(6) 6.8339(2) 33.2529(10) 90 95.272(3) 90 3564.6(2) 8 1.4857 0.648 1629.1 13159 6254 (0.0192) 6254/0/4401 1.055 0.0664, 0.1754	P-1 8.1644(6) 8.6556(6) 11.0961(9) 91.468(6) 93.665(7) 100.901(6) 767.84(10) 2 1.511 0.567 360.0 4871 2848 (0.01) 2848/0/199 0.941 0.0384, 0.1	38)
Crystal system Space group $a/Å$ $b/Å$ $c/Å$ $\alpha/^{\circ}$ $\beta/^{\circ}$ $\gamma/^{\circ}$ Volume/ $Å^{3}$	P2 ₁ /c 15.7525(6) 6.8339(2) 33.2529(10) 90 95.272(3) 90 3564.6(2) 8 1.4857 0.648 1629.1 13159 6254 (0.0192) 6254/0/4401 1.055	P-1 8.1644(6) 8.6556(6) 11.0961(9) 91.468(6) 93.665(7) 100.901(6) 767.84(10) 2 1.511 0.567 360.0 4871 2848 (0.01) 2848/0/199	38)

of quantum chemical codes based on the B3LYP level of theory⁴¹ using Gaussian16 software.⁴² The molecular electrostatic potential was generated through a constant value of electron density. The molecular structure of the cation was optimized with 6-311G(d,p) basis set⁴³ in water using

the IEFPCM method.⁴⁴ The calculated frequencies were positive indicating that a definite absolute minimum was found on the potential energy surface. GaussView 05 software⁴⁵ was used for the visualization of molecular structures and analysis of obtained results.

Table 2. Hydrogen bonds (Å) and angles (deg.) in 1-5

D-HA	d(HA)	d(DA)	∠(DHA)	Symmetry codes
		1		
N1-HO1	2.0	2.827(7)	162.0	x, y, z
N3-HO3	2.05	2.910(7)	169.0	$x, 3/2 - y, -\frac{1}{2} + z$
N4-HO3	1.93	2.782(7)	174.0	$x, 3/2 - y, -\frac{1}{2} + z$
C2-HO1	2.48	3.323(8)	136	$x, \frac{1}{2} - y, -\frac{1}{2} + z$
C7-HO1	2.43	3.073(9)	127	$x, 3/2 - y, -\frac{1}{2} + z$
		2		
N1-H···O4	2.05	2.876(9)	150	x, y, z
N3-H···O1	2.12	2.950(8)	163	x, y, z
N4-H···O1	1.9	2.736(8)	165	x, y, z
O4-H···O4	2.08	2.916(8)	167	$\frac{1}{2} + x$, $\frac{1}{2} - y$, $1 - z$
O4-H···O2	2.08	2.904(7)	163	$\frac{1}{2} - x$, $1 - y$, $-\frac{1}{2} + z$
N5-H···S1	2.71	3.479(6)	149	x , $\frac{1}{2} + y$, $\frac{3}{2} - z$
		3		
N1-H···Cl1	2.4	3.222(3)	160	$-\frac{1}{2} + x$, $\frac{3}{2} - y$, $1 - z$
N4-H···Cl1	2.29	3.081(3)	153	x, y, z
N3-H···Cl1	2.52	3.278(3)	148	x, y, z
C2-H···Cl1	2.78	3.563(3)	143	$-\frac{1}{2} + x$, $\frac{3}{2} - y$, $1 - z$
C10-H···S1	2.85	3.806(5)	146	$\frac{1}{2} - x$, $-\frac{1}{2} + y$, z
		4		
N1-H···Ow	1.95	2.7961(1)	166	<i>x</i> , <i>y</i> , <i>z</i>
N3-H···O4	2.41	3.1780(1)	150	x, y, z
Ow1-H···O6	2.03	2.8652(1)	168	1 - x, $2 - y$, $-z$
N4-H···O4	1.98	2.7580(1)	165	x, y, z
Ow1-H···O1	1.89	2.7198(1)	165	1 - x, $1 - y$, $-z$
N1a-H···Ow1	1.83	2.7826(1)	170	x, y, z
Ow-H···O3	1.89	2.7399(1)	172	x, y, z
Ow-H···O4	2.07	2.8977(1)	165	x, -1 + y, z
N3a-H···O6	2.47	3.2400(1)	149	1 - x, $1 - y$, $-z$
N4a-H···O6	1.93	2.7363(1)	162	1 - x, $1 - y$, $-z$
C2a-H···Ow1	2.58	3.3119(1)	136	<i>x</i> , <i>y</i> , <i>z</i>
		5		
N1-HO2	2.03	2.848(2)	158	x, 1 + y , z
N3-HO1	2.13	2.946(2)	157	1 - x, $1 - y$, $1 - z$
N4-HO1	1.86	2.687(2)	161	1 - x, $1 - y$, $1 - z$

3. Results and Discussion

Six new compounds **1–6** were synthesized in two steps. In the first step, 2-formylpyridine N^4 -allylthiosemicarbazone was obtained by the reaction between N^4 -allyl-3-thiosemicarbazide and 2-formylpyridine in ethanol. In the second step, 2-formylpyridine N^4 -allylthiosemicarbazone reacted with corresponding acids to form different salts. Single crystals of complexes **1–5** were obtained by recrystallization from ethanol. Elemental analysis was performed for all compounds, the results of which confirm the formula determined from the structure. The molar conductivity values of the synthesized compounds **1–6** are in the range $61–88~\Omega^{-1}\cdot\text{cm}^2\cdot\text{mol}^{-1}$, indicating that they behave as 1:1 electrolytes in solution.

In order to determine the changes that appear upon protonation of the thiosemicarbazone \mathbf{HL} , a comparative analysis of the NMR spectra of 2-formylpyridine N^4 -allylthiosemicarbazone, which is described in the literature, 30 and its nitric acid salt (1, Figures S2, S3) was performed. The protonation of the thiosemicarbazone \mathbf{HL} led to an increase of chemical shift values of the protons from the pyridine moiety, which can indicate the protonation of the pyridine nitrogen atom.

3. 1. Structural Study of Compounds 1-5.

The X-ray structures of compounds 1-5 are presented in Figures 1-6. The structures of these compounds consist of a protonated ligand H_2L^+ , solvent molecules (in the

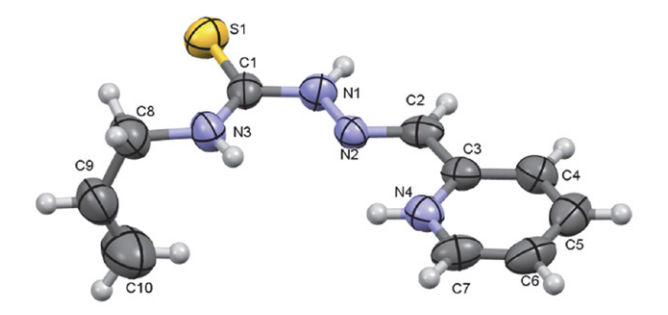


Figure 1. View of compounds with atom numbering. Thermal ellipsoids are drawn at a 50% probability level.

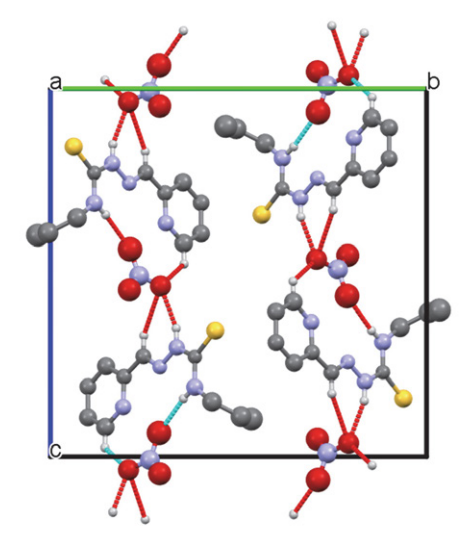


Figure 2. The crystal packing fragment of **1** with chains formation along the *c*-axis.

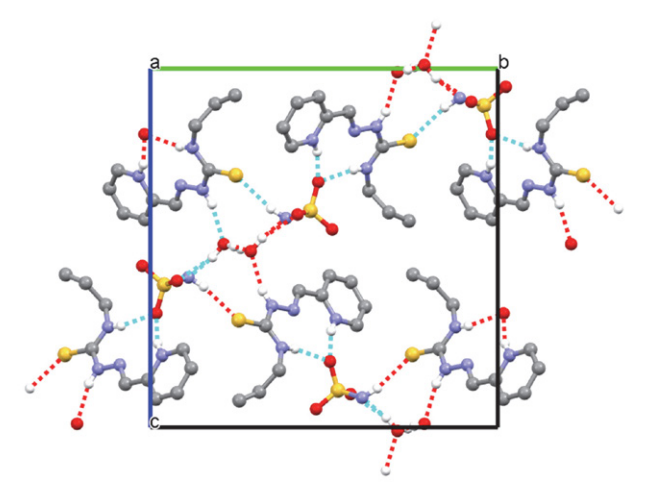


Figure 3. The fragment of *3D* supramolecular network in **2**.

case of **2**, **4**) and counter ions NO_3^- , $NH_2SO_3^-$, Cl^- , Cl_3CCOO^- , Cl_2CHCOO^- in **1–5** respectively. In **H**₂**L**⁺ (Figure 1a, Table S1) the substituents at N1–C1 bond are in the *E* position. In compounds **1–5**, the *A* (S1–N1–N2–N3–C1–C2) core is practically planar within 0.05 Å and the dihedral angles between *A* and pyridine ring range

from 2.2 to 10.7° . Meanwhile, the cation is nonplanar in studied compounds because the C3H5 substituent in the thiosemicarbazone moiety, the dihedral angles between the best planes of A and allyl groups lie in interval 71.5–83.8°. The bond lengths and angles, as well as the aforementioned values, are in good agreement with those in neutral molecules of 2-formyl-, 3-formyl-, and 4-formylpyridine N^4 -allylthiosemicarbazones.³⁰

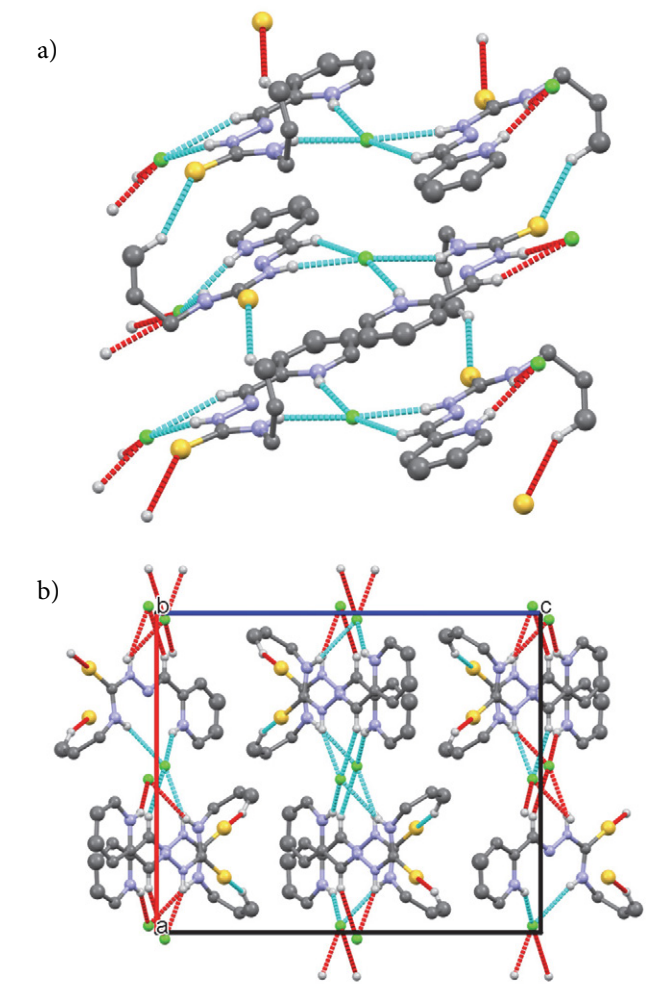


Figure 4. (a) Chains formation along b-direction via C10–H···S1 hydrogen bond; (b) fragment of layers in the crystal packing of 3, where chains are joined by chlorine atoms.

The presence of anions (in substances 1-5) and solvent molecules (in substances 2 and 4) affects the architecture of hydrogen bonds in their crystal structures. In the crystal of 1, the cations are joined by nitrato groups into the chains along the c-axis (Table 2, Figure 2). In the crystal of 2, the 3D supramolecular network is formed by hydrogen-bonding interactions involving the ligands H_2L^+ and solvent molecules (Figure 3). In 3 the ligands are linked by C10–H···S1 hydrogen bonds in chains along the b-direction. In turn, these chains are joined by chlorine at-

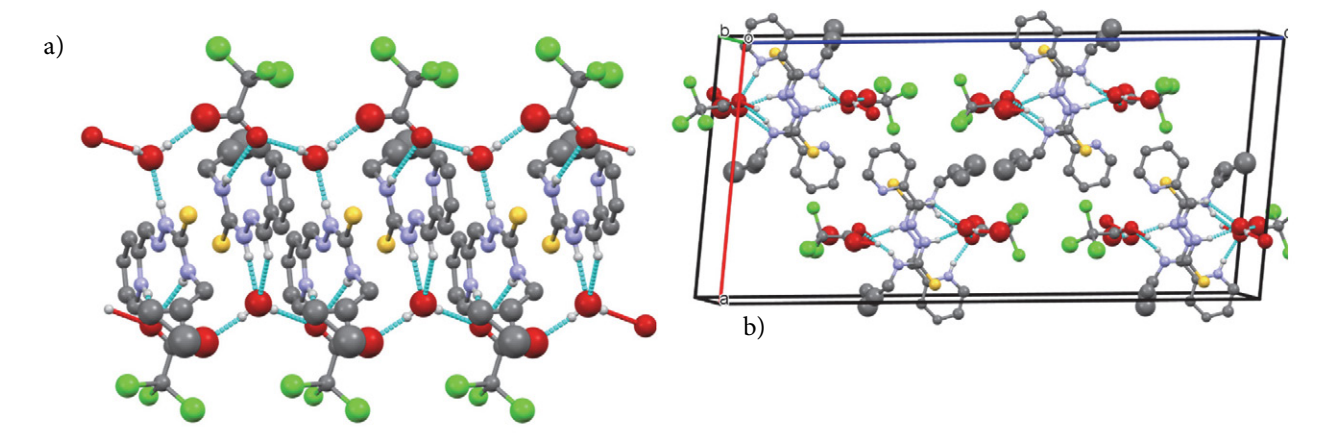


Figure 5. (a) Formation of chains along the *b*-axis through hydrogen bonds involving water molecules and anions; (b) fragment of crystal packing in 4

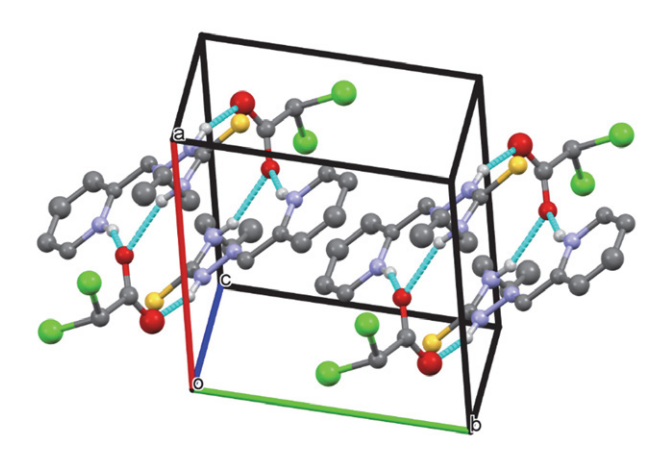


Figure 6. The centrosymmetric dimers in 5, where monomers are held together by bridge solvent molecules.

oms into layers parallel to the (001) plane (Figure 4a, b). In 4 the cations form the chains along the *b*-axis *via* hydrogen bonds with two water molecules and anions (Figure 5a, b). In the crystal of 5, the cations form the centrosymmetric dimers where the monomers are held together by bridge solvent molecules through hydrogen bonds (Figure 6). Between chains in 1 and 4, layers in 3, and dimers in 5 occur the van der Waals interactions.

3. 3. Antiradical Activity

The antiradical activity of the compounds 1–6 was determined by the ABTS*+ method (Table 3). In all cases, the obtained salts manifest a higher antiradical activity than the initial thiosemicarbazone **HL**.³⁰ The IC₅₀ values of the obtained salts 1–6 are 5–30% lower than that of non-protonated thiosemicarbazone. Based on the presented results we can conclude that the acidic residue in the composition of the thiosemicarbazone salts also has an influence on its antiradical activity. The antiradical activity of the studied compounds decreases according to the fol-

lowing series of dependences of acid residues: $\text{Cl}^- > \text{Cl}_2\text{CHCOO}^- > \text{Cl}_3\text{CCOO}^- > \text{NO}_3^- \approx \text{SO}_3\text{NH}_2^- > \text{ClCH}_2\text{COO}^-$. All the studied substances showed activity higher than Trolox, a standard antioxidant used for antioxidant capacity assays. Compound [H₂L]Cl (3) showed the greatest activity with an IC₅₀ value of 9.9 μ mol/L, being three times more active than Trolox.

Compared with the literature data we have previously published,⁴⁰ the 2-acetylpyridine 4-allylthiosemicarbazone showed no antiradical activity, leading to conclusion that the presence of a 2-formylpyridine fragment in the structure of thiosemicarbazone enhances its antiradical activity.

Table 3. Antiradical activity of the studied substances in terms of IC₅₀ values toward ABTS*+

Compound	$ m IC_{50}$, $ m \mu mol/L$		
HL	14.2±1.8		
1	12.9±0.4		
2	12.9±1.0		
3	9.9±1.0		
4	12.1±0.7		
5	10.9±0.9		
6	13.4±0.8		
Trolox	33.0±0.7		

3. 3. DFT Calculations

It is known that the frontier molecular orbitals (FMOs) such as the highest occupied molecular orbitals (HOMO) and lowest unoccupied molecular orbitals (LU-MO) may act as electron donors and acceptors, respectively. The energies of FMOs are used for the calculation of molecular descriptors which are important parameters for the characterization of the reactivity of molecules. The definition and detailed analysis of molecular descriptors and FMOs of neutral **HL** were done previously.^{30,46} The

contour plot of the ground state FMOs of cation is shown in Figure 2. The energy gaps between HOMO and LUMO in H₂L⁺ and HL are different, being 2.04 and 3.771 eV, respectively. However, the composition of frontier molecular orbitals of these molecules is very similar. The HOMOs of H₂L⁺ and HL are located mainly on the sulphur atoms with a small contribution of nitrogen atoms of the chains, while the LUMOs are distributed in thiosemicarbazone moieties and pyridine rings. Meanwhile, the molecular descriptors, namely electronegativity (χ), chemical hardness (η), and electrophilic index (ω) are significantly different in cations and neutral molecule. Compounds with high electronegativity are less likely to donate electrons. The lowest the chemical hardness value, the highest the activity of a molecule. The lowest electrophilic index is characterized by the highest electron donation ability. The values of χ , η , and ω for H_2L^+ and HL are 8.033, 1.02, 31.638 eV and 3.767, 1.886, 3.763 eV, respectively, and the main difference among these quantities is related to electronegativity and electrophilic index.

The molecular electrostatic potential (MEP) surface of $\mathbf{H}_2\mathbf{L}^+$ was mapped, using the optimized geometries (Figure 3). The MEPs of cations and neutral molecule are significantly different. The values of MEPs in $\mathbf{H}_2\mathbf{L}^+$ range from 0.0 to 62.75 kcal/mol, while in $\mathbf{H}\mathbf{L}$ the MEP increase in the order -31.7 kcal mol⁻¹ = red < yellow < green < blue = 31.7 kcal mol⁻¹. In the last compound, the negative (red and yellow) regions of MEP are related to electrophilic reactivity

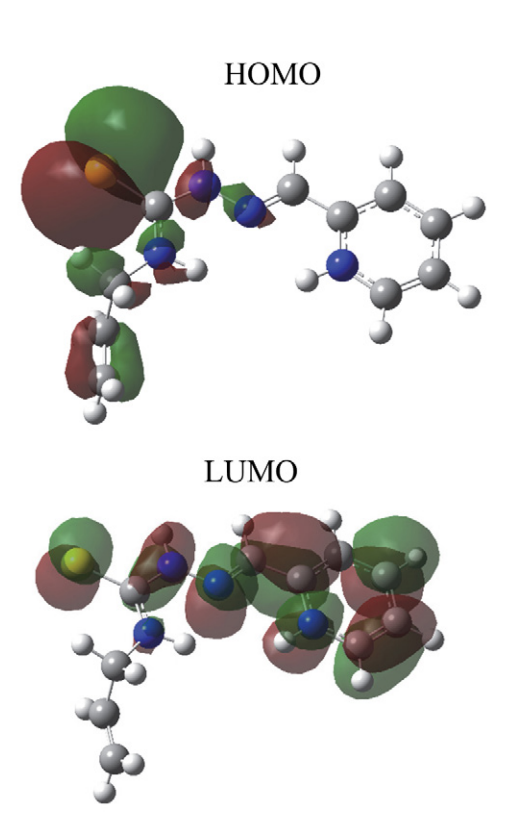


Figure 7. View of HOMO and LUMO of the studied molecule.

and the positive (blue) regions to nucleophilic reactivity whereas in $\mathbf{H}_2\mathbf{L}^+$ the molecular electrostatic potential is positive and corresponds to nucleophilic reactivity only.



Figure 8. Electrostatic potentials mapped on the molecular surfaces of the studied molecule. The values of MEPs range from 0.0 to 62.75 kcal/mol.

Thus, the difference in molecular descriptors and molecular electrostatic potentials of $\mathbf{H}_2\mathbf{L}^+$ and $\mathbf{H}\mathbf{L}$ may indicate different mechanisms of their antioxidant activity because the electronic structure of the cation is more favorable for accepting electrons if compared with $\mathbf{H}\mathbf{L}$.

4. Conclusions

We have described in this paper synthesis of six salts of 2-formylpyridine N^4 -allylthiosemicarbazone with nitric, hydrochloric, chloroacetic, dichloroacetic, trichloroacetic and sulfaminic acids, and crystal structure of five of them, as well as their antiradical activity toward ABTS*+ and compared them with the activity of neutral molecule of 2-formylpyridine N^4 -allylthiosemicarbazone and Trolox. Protonation of the thiosemicarbazone moiety led to an increase in antiradical activity. The corresponding IC50 values became lower by 5–30%.

Protonation of the pyridine fragment in this thiosemicarbazone induces changes in the molecular electrostatic potential surface and molecular descriptors, including electronegativity, chemical hardness, and electrophilic index. These alterations make the cation $\mathbf{H_2L^+}$ more favorable for accepting electrons and thus contribute to the change in antiradical activity. Thus, all of the obtained salts manifest higher antiradical activity, which also depends on the nature of the acid moiety. The most active one is the salt with chloride anion, then the one with the dichloroacetate anion. So, the transformation of thiosemicarbazones into salts in this case leads to an increase in antiradical activity, and the continuation of this study on other N-substituted thiosemicarbazones represents an interest for enhancing antiradical activity of this important class of bioactive substances.

Acknowledgments

This work was fulfilled with the financial support of the subprograms 010602 and 010701.

Supplementary Materials

CCDC 2270394-2270398 contains the supplementary crystallographic data for the compounds 1-5. Copies of the data can be obtained free of charge on application to CCDC, 12 Union Road, Cambridge CB2 1EZ, UK (fax: 44-1223-336-033; e-mail:deposit@ccdc.cam.ac.uk or www.http://www.ccdc.cam.ac.uk)

5. References

- S. Vertuani, A. Angusti, S. Manfredini, Curr. Pharm. Des. 2004, 10, 1677–1694. DOI:10.2174/1381612043384655
- R. Mittler, *Trends Plant Sci.* 2002, 7, 405–410.
 DOI:10.1016/S1360-1385(02)02312-9
- B. Halliwell, R. Aeschbach, J. Löliger, O. I. Aruoma, Food Chem. Toxicol. 1995, 33, 601–617.
 DOI:10.1016/0278-6915(95)00024-V
- 4. O. E. Ifeanyi, Int. J. Curr. Res. Med. Sci 2018, 4, 123-133.
- 5. K. J. Davies, *IUBMB Life* **2000**, *50*, 279–289. **DOI:**10.1080/15216540051081010
- 6. H. Sies, Eur. J. Biochem. 1993, 215, 213–219. DOI:10.1111/j.1432-1033.1993.tb18025.x
- F. Gagne: Biochemical Ecotoxicology Principles and Methods, Elsevier Academic Press Inc., 2014, pp. 103–115.
 DOI:10.1016/B978-0-12-411604-7.00006-4
- A. Phaniendra, D. B. Jestadi, L. Periyasamy, *Indian J. Clin. Biochem.* 2015, 30, 11–26. DOI:10.1007/s12291-014-0446-0
- 9. L. He, T. He, S. Farrar, L. Ji, T. Liu, X. Ma, *Cell Physiol. Biochem.* **2017**, *44*(2), 532–553. **DOI:**10.1159/000485089
- C. Bonaccorso, T. Marzo, D. La Mendola, *Pharmaceuticals* 2019, 13, 4. DOI:10.3390/ph13010004
- 11. L. Yang, H. Liu, D. Xia, S. Wang, *Molecules* **2020**, *25*, 1192. **DOI:**10.3390/molecules25051192
- 12. D. S. Kalinowski, P. Quach, D. R. Richardson, *Future Med. Chem.* **2009**, *1*, 1143–1151. **DOI:**10.4155/fmc.09.80
- 13. M. A. Metwally, S. Bondock, H. El-Azap, E. E. M. Kandeel, *J. Sulphur Chem.* **2011**, *32*, 489–519.
 - DOI:10.1080/17415993.2011.601869
- N. P. Prajapati, H. D. Patel, Synth. Commun. 2019, 49, 2767– 2804.
- F. Kanso, A. Khalil, H. Noureddine, Y. El-Makhour, *Int. Immunopharmacol.* 2021, 96, 107778.
 DOI:10.1016/j.intimp.2021.107778
- P. F. Rapheal, E. Manoj, M. P. Kurup, *Polyhedron* 2007, 26, 818–828. DOI:10.1016/j.poly.2006.09.091
- M. N. M. Milunović, O. Palamarciuc, A. Sirbu, S. Shova, D. Dumitrescu, D. Dvoranová, P. Rapta, T. V. Petrasheuskaya, E. A. Enyedy, G. Spengler, M. Ilic, H. H. Sitte, G. Lubec, V. B. Arion, *Biomolecules* 2020, 10, 1213.
 - DOI:10.3390/biom10091213
- 18. S. Arora, S. Agarwal, S. Singhal, *Int. J. Pharm. Sci.* **2014.**, 6, 34–41.
- E. J. Siddiqui, I. Azad, A. R. Khan, T. Khan, JDDT 2019, 9, 689–703. DOI:10.22270/jddt.v9i3.2888
- 20. S. Gupta, N. Singh, T. Khan, S. Joshi, Results Chem. 2022, 4,

- 100459. DOI:10.1016/j.rechem.2022.100459
- A. B. Ibrahim, M. K. Farh, S. A. El-Gyar, M. A. El-Gahami, D. M. Fouad, F. Silva, I. C. Santos, A. Paulo, *Inorg. Chem. Commun.* 2018, 96, 194–201. DOI:10.1016/j.inoche.2018.08.023
- S. Chandra, S. Parmar, Y. Kumar, Bioinorg. Chem. Appl. 2009, 851316.
- A. P. Gulea, K. S. Lozan-Tyrshu, V. I. Tsapkov, I. D. Korzha, V. F. Rudik, *Russ. J. Gen. Chem.* 2012, 82, 1869–1872.
 DOI:10.1134/S1070363212110242
- D. X. West, D. L. Huffman, J. S. Saleda, A. E. Liberta, *Transition Met. Chem.* 1991, 16, 565–570. DOI:10.1007/BF01024187
- D. X. West, J. S. Saleda, A. E. Liberta, *Transit. Met. Chem.* 1991, 17, 568–572. DOI:10.1007/BF02910760
- 26. G. Atassi, P. Dumont, J. C. E. Harteel, *Eur. J. Cancer* **1979**, *15*, 451–459. **DOI**:10.1016/0014-2964(79)90080-X
- E. W. Ainscough, A. M. Brodie, J. D. Ranford, J. M. Waters, J. Chem. Soc. 1991, 2125–2131.
- K. C. Agrawal, B. A. Booth, S. M. DeNuzzo, A. C. Sartorelli, J. Med. Chem. 1976, 19, 1209–1214.
 DOI:10.1021/jm00232a008
- D. C. Ilies, S. Shova, V. Radulescu, E. Pahontu, T. Rosu, *Polyhedron* 2015, 97, 157–166. DOI:10.1016/j.poly.2015.05.009
- V. Graur, Y. Chumakov, O. Garbuz, C. Hureau, V. Tsapkov, A. Gulea, *Bioinorg. Chem. Appl.* 2022, 2022.
 DOI:10.1155/2022/2705332
- 31. J. Fries, H. Getrost: Organic Reagents for Trace Analysis, E. Merck Darmstadt, Germany, 1977.
- 32. W. Zhao, M. Zhao, Chin. J. Org. Chem. 2001, 21, 681.
- 33. B. M. Zeglis, V. Divilov, J. S. Lewis, *J. Med. Chem.* **2011**, *54*, 2391–2398. **DOI**:10.1021/jm101532u
- O. V. Dolomanov, L. J. Bourhis, R. J. Gildea, J. A. K. Howard, H. Puschmann, J. Appl. Cryst. 2009, 42, 339–341.
 DOI:10.1107/S0021889808042726
- 35. G. M. Sheldrick, *Acta Crystallogr.*, *Sect. A: Found. Crystallogr.* **2008**, 64, 112–122. **DOI:**10.1107/S0108767307043930
- G. M. Sheldrick, Acta Crystallogr., Sect. C: Struct. Chem.
 2015, 71, 3. DOI:10.1107/S2053229614024218
- A. L. Spek, Acta Crystallogr. D65 2009, 148–155.
 DOI:10.1107/S090744490804362X
- C. F. Macrae, P. R. Edgington, P. McCabe, E. Pidcock, G. P. Shields, R. Taylor, M. Towler, J. van De Streek, *J. Appl. Cryst.* 2006, 39, 453–457. DOI:10.1107/S002188980600731X
- R. Re, N. Pellegrini, A. Proteggente, A. Pannala, M. Yang, C. Rice-Evans, *Free Radicals Biol. Med.* 1999, 26, 1231–1237.
 DOI:10.1016/S0891-5849(98)00315-3
- V. Graur, I. Usataia, P. Bourosh, V. Kravtsov, O. Garbuz, C. Hureau, A. Gulea, *Appl. Organomet. Chem.* 2021, 35, e6172.
 DOI:10.1002/aoc.6172
- 41. C. Lee, W. Yang, R. G. Parr, *Phys. Rev.* **1988**, *B. 37*, 785–789. **DOI:**10.1103/PhysRevB.37.785
- 42. M. J. Frisch, G. W. Trucks, H. B. Schlegel, G. E. Scuseria, M. A. Robb, J. R. Cheeseman, G. Scalmani, V. Barone, G. A. Petersson, H. Nakatsuji, X. Li, Gaussian 16 Search PubMed. Gaussian Inc., Wallingford, CT, 2016.
- 43. E. V. R. Castro, F. E., J. Jorge, *Chem. Phys.* **1998**, *108*, 5225–5229. **DOI**:10.1063/1.475959

- 44. D. M. Chipman, Theor. Chem. Acc. 2002, 107, 80–89. DOI:10.1007/s00214-001-0302-1
- 46. Z. Lakbaibi, H. Abou El Makarim, M. Tabyaoui, A. El Hajbi, J. Mater. Environ. Sci. 2016, 8, 99–115.
- 45. R. Dennington, T. Keith, J. Millam, Gauss View 2009, Version
 - 5. Semichem Inc., Shawnee Mission.

Povzetek

Sintetizirali smo šest novih 2-formilpiridin N^4 -aliltiosemikarbazonskih soli ([H₂L]X·nH₂O, kjer je X NO₃⁻ (1), NH₂SO₃⁻ (2), Cl⁻ (3), Cl₃CCOO⁻ (4), Cl₂CHCOO⁻ (5), ClCH₂COO⁻ (6); n = 0 (1, 3, 5, 6), 1 (2, 4)) in določili njihove fizikalne ter kemijske lastnosti s pomočjo elementne analize, meritev prevodnosti, FT-IR ter ¹H in ¹³C NMR spektroskopije. Kristalne strukture spojin 1–5 smo določili s pomočjo rentgenske difrakcije na monokristalu. Podatki kristalne analize kažejo, da so strukture spojin sestavljene iz protonirane oblike tiosemikarbazonov $\mathbf{H}_2\mathbf{L}^+$, ustreznega aniona (kislinskega ostanka) in molekule vode (v primerih 2 in 4). Te spojine izkazujejo antiradikalsko aktivnost proti ABTS^{*+} kation radikalu, ki presega aktivnost neprotoniranega izhodnega tiosemikarbazona $\mathbf{H}_2\mathbf{L}$ in tudi Troloksa, ki se standardno uporablja za medicinske namene. Najbolj aktivna spojina je [H₂L]Cl (3) z IC₅₀ vrednostjo 9.9 µmol/L. Izračuni s teorijo gostotnega potenciala kažejo, da je elektronska struktura kationa $\mathbf{H}_2\mathbf{L}^+$ bolj dovzetna za sprejemanje elektronov kot pa $\mathbf{H}_2\mathbf{L}$.



Except when otherwise noted, articles in this journal are published under the terms and conditions of the Creative Commons Attribution 4.0 International License